APC is required for muscle stem cell proliferation and skeletal muscle tissue repair

Alice Parisi,[1,2] Floriane Lacour,[1,2] Lorenzo Giordani,[1,2] Sabine Colnot,[1,2] Pascal Maire,[1,2] and Fabien Le Grand[1,2]

[1]Institut Cochin, Université Paris-Descartes, Centre National de la Recherche Scientifique (CNRS), UMR 8104, 75014 Paris, France
[2]Institut National de la Santé et de la Recherché Médicale (INSERM) U1016, 75014 Paris, France

The tumor suppressor adenomatous polyposis coli (APC) is a crucial regulator of many stem cell types. In constantly cycling stem cells of fast turnover tissues, APC loss results in the constitutive activation of a Wnt target gene program that massively increases proliferation and leads to malignant transformation. However, APC function in skeletal muscle, a tissue with a low turnover rate, has never been investigated. Here we show that conditional genetic disruption of APC in adult muscle stem cells results in the abrogation of adult muscle regenerative potential. We demonstrate that APC removal in adult muscle stem cells abolishes cell cycle entry and leads to cell death. By using double knockout strategies, we further prove that this phenotype is attributable to overactivation of β-catenin signaling. Our results demonstrate that in muscle stem cells, APC dampens canonical Wnt signaling to allow cell cycle progression and radically diverge from previous observations concerning stem cells in actively self-renewing tissues.

Introduction

The *APC* gene codes for a large protein with multiple cellular functions and interactions (Fodde et al., 2001a; McCartney and Näthke, 2008; Nelson and Näthke, 2013). APC is an essential component of the canonical Wnt signaling pathway and is required for the formation of a cytoplasmic complex that targets β-catenin for proteasomal degradation when Wnt signals are absent (Clevers and Nusse, 2012). APC also participates in several cellular processes: cell adhesion and migration (Watanabe et al., 2004), actin dynamics (Moseley et al., 2007), and chromosome segregation (Fodde et al., 2001b). In humans, APC mutations lead to the second most common cause of cancer death (Morin et al., 1997). More specifically, in high turnover tissues, such as in the intestine, loss or mutation of APC leads to uncontrolled proliferation and accumulation of aberrant cells, thereby leading to carcinogenesis (Sansom et al., 2004; Andreu et al., 2005). Due to its role in controlling cell cycle progression of several stem cell compartments, APC was a good candidate to regulate muscle stem cell proliferation and quiescence, which to date are poorly characterized.

In adult skeletal muscle, a tissue with slow turnover, a pool of Pax7+ muscle stem cells called satellite cells ensures myofibers regeneration after injury (Seale et al., 2000; Lepper et al., 2011; Günther et al., 2013). Satellite cells are quiescent and lie under the basal lamina of their host muscle fibers unless activated upon injury. After exit from quiescence, satellite cells leave their niche, proliferate, and either differentiate to fuse and form new fibers or self-renew to replenish the stem cell niche (Yin et al., 2013). Although a diverse range of signals have been shown to regulate skeletal muscle regeneration, the molecular mechanism underlying cell cycle progression of muscle stem cells remains to be fully elucidated.

Results and discussion

Loss of APC does not perturb satellite cell quiescence

To understand APC function in adult regenerative myogenesis, we used inducible gene inactivation. The *APC* gene was conditionally deleted in satellite cells by crossing $APC^{flox/flox}$ mice (Colnot et al., 2004) with tamoxifen (TM)-inducible $Pax7^{CreERT2}$ mice (Lepper et al., 2009; termed APC SC-KO mice). After four daily TM injections in 2-mo-old animals (see Materials and methods; Fig. 1 A), we isolated by FACS and genotyped the satellite cells and the fibroblasts of tamoxifen-treated APC-SC-KO mice (Fig. 1 B). As expected, the APC-deleted specific band was detected only in satellite cells of APC-SC-KO mice but not in satellite cells of control mice. Notably, the APC-deleted band was absent in the fibroblast's genomic DNA (Fig. 1 B), thus confirming that APC gene disruption occurred selectively in satellite cells. We further observed the ab-

Correspondence to F. Le Grand: fabien.le-grand@inserm.fr

F. Lacour, L. Giordani, and F. Le Grand's present address is Myology Research Center, Sorbonne Universités, University Pierre et Marie Curie, UM76, 75013 Paris, France.

A. Parisi's present address is Nestlé Institute of Health Sciences SA, 1015 Lausanne, Switzerland.

Abbreviations used in this paper: EDL, extensor digitorum longus; PCNA, proliferating cell nuclear antigen; TM, tamoxifen.

The Rockefeller University Press $30.00
J. Cell Biol. Vol. 210 No. 5 717–726
www.jcb.org/cgi/doi/10.1083/jcb.201501053

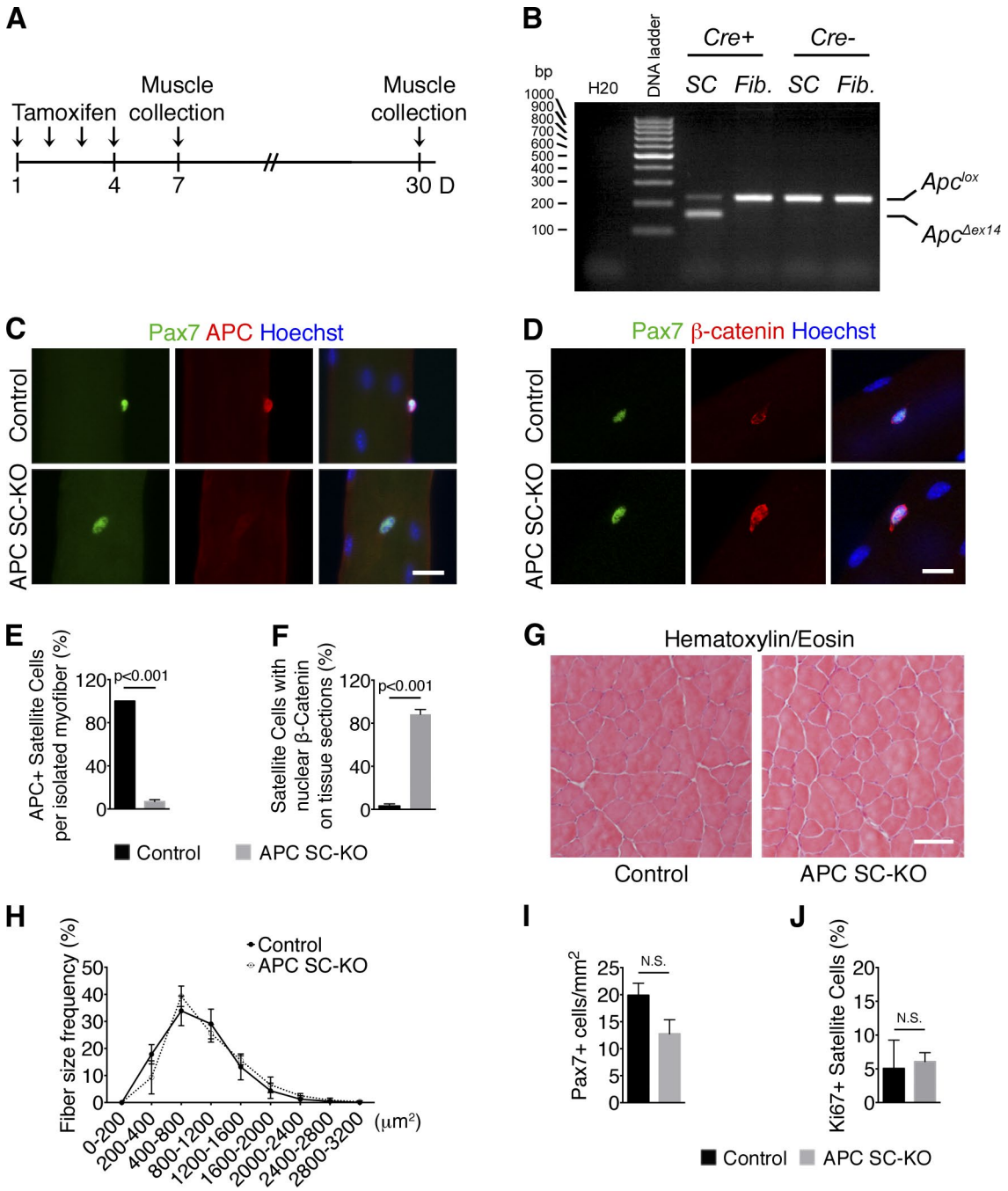

Figure 1. **Conditional APC gene disruption in the adult satellite cells does not affect skeletal muscle tissue integrity.** (A) Schematic representation of TM regimen and muscle collection for control (Pax7^{CreER}) and APC SC-KO (Pax7^{CreER};APC$^{lox/lox}$) mice. (B) PCR of gDNA extracted from FACS-sorted satellite cells (SC) and fibroblasts (Fib.) of TM-treated APC-floxed mice showing the accumulation of the *Apcdex14* band in satellite cells of mice that also express Pax7^{CreER}. (C and D) Immunostaining on single EDL myofibers isolated 3 d after TM treatment. APC immunostaining (C) demonstrates efficient loss of APC expression in satellite cells (Pax7+) of APC SC-KO mice. β-Catenin immunostaining (D) shows that β-catenin is stabilized after APC knockout. (E and F) Quantification of the percentage of APC+ satellite cells on isolated EDL myofibers and the percentage of satellite cells with nuclear β-catenin on TA cryosections. Targeted APC gene disruption is efficient in vivo. (G) Hematoxylin and eosin staining on uninjured TA cryosections 30 d after TM treatment shows that tissue integrity is not altered after APC gene inactivation. (H) Distribution of myofibers cross-sectional area (CSA) shows no significant difference between uninjured TAs of control and APC SC-KO mice 30 d after TM treatment. (I and J) Quantification of the total number of satellite cells/mm^2 (I) and of the proportion of ki67+ proliferating satellite cells (J) reveal that muscle stem cell quiescence is not perturbed upon APC loss. Bars: (C and D) 10 µm; (G) 50 µm. Nuclei are stained with Hoechst. Error bars indicate SEM. N.S., not significant ($P > 0.05$).

sence of APC protein (Fig. 1 C) and the nuclear accumulation of β-catenin protein (Fig. 1 D) in satellite cells of APC SC-KO extensor digitorum longus (EDL) single myofibers, 1 wk after the first TM injection. Efficient APC genetic disruption was observed in the vast majority of satellite cells after induction of Cre activity both on isolated myofibers (Fig. 1 E) and on tissue sections (Fig. 1 F).

We did not observe any alterations of skeletal muscles gross anatomy 1 mo after TM treatment. Uninjured tibialis anterior (TA) muscles of APC SC-KO mice appeared undistinguishable

from controls at the histological level (Fig. 1 G), and muscle fiber size remained constant (Fig. 1 H). APC loss did not lead satellite cells to leave their quiescent state, since both control and APC SC-KO TA muscles exhibited similar numbers of sublaminar Pax7+ satellite cells (Fig. 1 I) and a very low proportion of Ki67+ cycling satellite cells (Fig. 1 J). Collectively, our observations indicate that APC gene disruption does not result in muscle satellite cell exit from quiescence or in their malignant transformation.

Conditional APC gene disruption in satellite cells results in complete failure of muscle regeneration

To determine if APC mutant satellite cells can support injury-induced myogenesis, we injured TA muscles by cardiotoxin injection (Chang et al., 1972; Fig. 2 A). The early satellite cell–dependent events of regenerative myogenesis were abrogated after APC loss, as indicated by the total absence of accumulating Pax7+ progenitors (Fig. 2 B) and of newly formed myofibers expressing embryonic myosin heavy chains (e-MyHC; Fig. 2 C) 4 d after injury. 2 wk after injury, control muscles were fully regenerated and composed of functional myofibers (1,629 ± 278 regenerated myofibers/mm^2), whereas APC SC-KO muscles dramatically failed to regenerate (9 ± 7 regenerated myofibers/mm^2; Fig. 2 D), with the remaining tissue accounting for less than half the contralateral uninjured muscle weight (Fig. 2 E). Hematoxylin and eosin staining at different time points after CTX injection (ranging from 2 d to 28 d after injury) confirmed the inability of APC SC-KO muscle to regenerate (Fig. S1). In APC SC-KO mice, muscle tissue was replaced by a scar tissue composed of Tcf4+ fibroblasts (Fig. 2, F and G) and a Collagen Type I matrix (Fig. 2, H and I). To rule out the possibility that the excessive Tcf4+ cells derived from mutant satellite cells that lost their identity, we performed regeneration assays in mice bearing the double-reporter Z/EG lineage tracing allele (Novak et al., 2000). In these mice, Cre activity results in the permanent expression of the EGFP in targeted cells and their descendants. In control conditions, all regenerated myofibers derived from the Pax7 lineage, whereas APC SC-KO muscles did not contain EGFP+ cells (Fig. 2 K). Furthermore, we did not detect any Pax7+ cells in APC SC-KO TAs 14 d after injury (Fig. 2 L), indicating that adult-specific APC mutant satellite cells cannot self-renew and repopulate the niche (Fig. 2 J). Thus, APC expression by satellite cells is required for injury-induced myogenesis.

APC is required for satellite cell survival

To determine whether the observed phenotype was cell-intrinsic or depended on the muscle microenvironment, we tried unsuccessfully to grow in vitro satellite cell–derived primary myoblasts isolated from APC SC-KO muscles using a widely used protocol that routinely works in our hands (Fig. 3 A). We then isolated single myofibers with their associated satellite cells from EDL muscle and plated them on Matrigel. In these conditions, satellite cells leave their niche and migrate away from the fibers to generate myogenic colonies. Compared with controls, APC-inactivated satellite cells were defective in expansion and failed to establish myogenic colonies (Fig. 3, B and C). To identify the cellular events involved in this process, we studied satellite cell behavior in their niche at the surface of isolated single myofibers in "floating" culture conditions (Fig. 3 D). We observed that mutant satellite cells did not incorporate BrdU and did not divide after 24 h and 30 h of culture (Fig. 3, E and F, respectively). As a consequence, while the number of myofiber-associated satellite cells was not different between control and APC SC-KO myofibers directly after isolation, APC mutant satellite cells were unable to amplify and give rise to Pax7+ cells clusters (Fig. 3 G). More specifically, we observed that satellite cells of APC SC-KO myofibers expressed the active form of Caspase-3 (Fig. 3, H and I), indicating that they were undergoing programmed cell death. Importantly, we did not observe accelerated differentiation (Myogenin+ cells) in APC mutant satellite cells (Fig. 3 J). To test whether cell cycle arrest and programmed cell death are responsible for the regeneration failure of APC SC-KO mice, we performed BrdU incorporation assays after cardiotoxin injury and analyzed satellite cells at the earliest time point in vivo (48 h after injury; Fig. 3 K). We observed that, in contrast to control satellite cells, APC mutant satellite cells did not incorporate BrdU, demonstrating that they do not enter into S phase in vivo (Fig. 3 L). TUNEL staining further revealed an increase in the number of apoptotic cells in APC SC-KO muscles compared with controls (Fig. 3 M). Collectively, our results suggest that APC is necessary for satellite cell survival at the time of exit from quiescence.

To understand the molecular mechanisms underlying the requirement of APC by satellite cells, and because APC SC-KO satellite cells did not grow in vitro, we silenced APC in proliferating wild-type satellite cell–derived primary myoblasts (Fig. S2 A) and analyzed global gene expression 48 h after transfection using Affymetrix mRNA microarrays. APC knockdown led to down-regulation of 337 and up-regulation of 291 transcripts relative to mock-treated cells, with a false discovery rate (FDR) of <5% (Table S2). Differentially expressed genes had enriched gene ontology terms belonging to regulatory pathways associated with nucleotide binding, chromosomes, and cell cycle (Table S1). Ingenuity pathway analysis demonstrated enrichment of the programmed cell death pathway along with reduction of the cell cycle, cellular assembly, and DNA replication pathways (Fig. S2 B). Overall, changes in gene expression were consistent with apoptosis of APC-deficient primary myoblasts and indicated a link with impaired cell cycle progression. More specifically, we observed that transcription of proliferating cell nuclear antigen (PCNA) and several factors that associate with PCNA during DNA replication were down-regulated after APC silencing (Fig. S2 C). On single myofibers, quiescent satellite cells do not express PCNA whereas almost all activated satellite cells express high levels of PCNA proteins (Fig. S2 D). APC mutant satellite cells were unable to express PCNA proteins (Fig. S2 E), and in these conditions PCNA silencing on single myofibers impaired satellite cell amplification, similarly to APC silencing (Fig. S2 F).

APC allows satellite cell progression through the cell cycle by dampening canonical Wnt signaling

We next aimed to understand which signaling cascade could explain the observed phenotype. By analyzing our microarray data with the Upstream Regulators tool of the Ingenuity software, we identified WNT3A as one of the pathways activated after APC silencing (Fig. S3 A). Indeed, 23 known canonical Wnt target genes were up-regulated in APC-depleted primary myoblasts (Fig. S3 B). We then determined the activation status of canonical Wnt signaling in satellite cells ex vivo and in vivo. We found that β-catenin was uniquely cytoplasmic (inactive signaling) in quiescent satellite cells and in satellite cells undergoing their

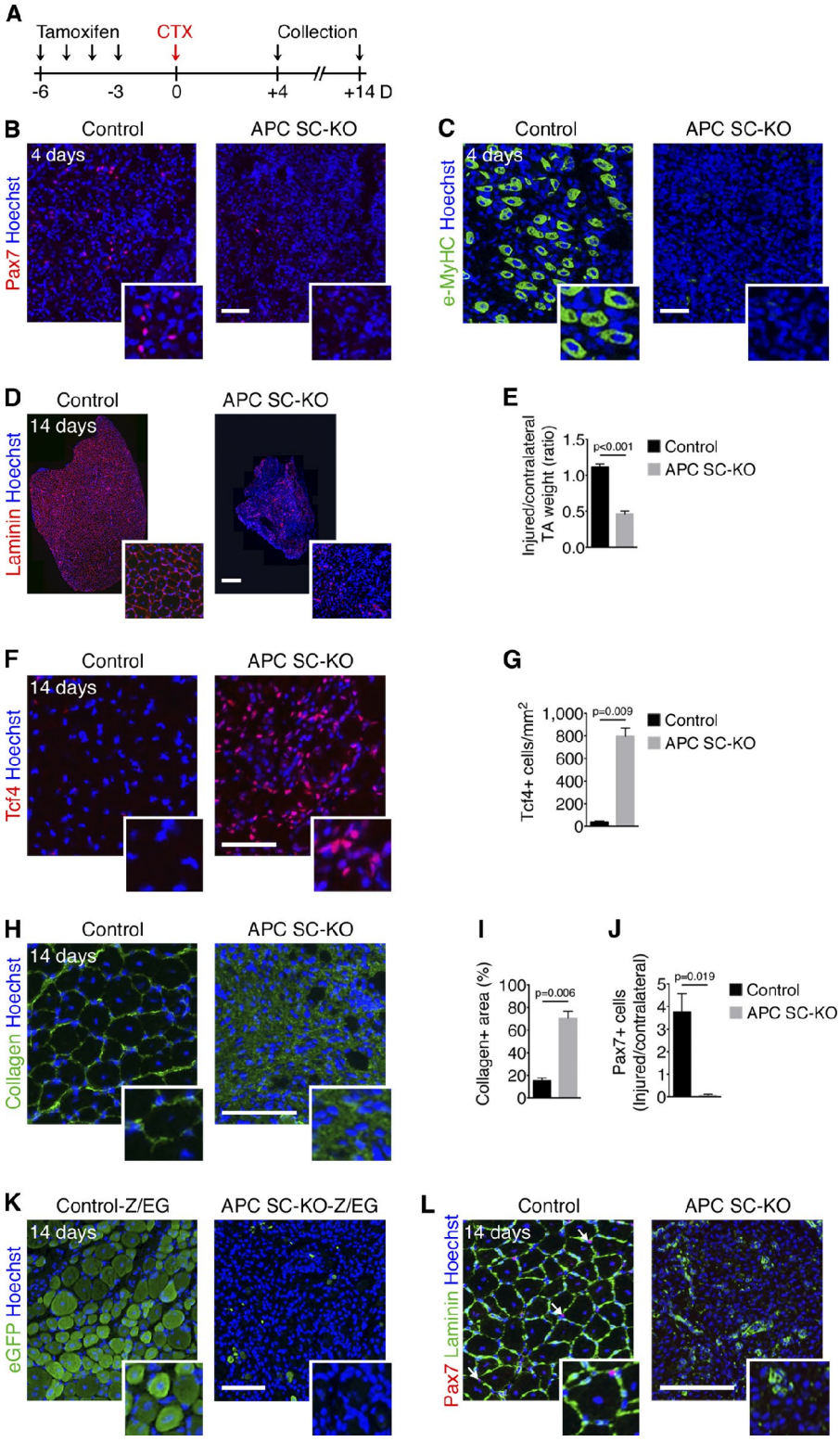

Figure 2. **APC is required for adult skeletal muscle regeneration.** (A) TM regimen and cardiotoxin (CTX) injury scheme for control and APC SC-KO mice. (B and C) Immunostaining for Pax7 (B) and e-MyHC (C) on TA cryosections 4 d after injury. (D–L) Analysis of TA muscles 14 d after injury reveals that tissue regeneration is defective in APC SC-KO muscles. (D) Whole sections of TA muscles immunostained for Laminin. Immunostaining for Tcf4 (F), type 1 Collagen (H), and Pax7 and Laminin (L) on TA cryosections is shown. Quantification of TA weight 14 d after injury normalized by uninjured TA weight (E), of the number of Tcf4+ cells/mm^2 (G), of relative Collagen+ area (I), and of sublaminar Pax7+ cells (normalized by Pax7+ cells of uninjured TA; J) is also shown. (K) GFP immunostaining on transverse sections of TAs isolated from Pax7^{CreER};Z/EG (Control-Z/EG) and Pax7^{CreER}APC$^{lox/lox}$;Z/EG (APC SC-KO-Z/EG) 14 d after injury demonstrates that APC-null satellite cells do not give rise to new myofibers, nor trans-differentiate in other cell types. Bars: (B, C, F, H, K, and L) 50 µm; (D) 200 µm. Nuclei are stained with Hoechst. Error bars indicate SEM. Inset panels show a 2× enlargement.

first division. However, strong β-catenin nuclear accumulation (active signaling) was detected in the progeny of satellite cells at the time of fate commitment and cell cycle exit (Fig. S3 C). Accordingly, expression of the Wnt reporter allele Axin2^{LacZ} (Lustig et al., 2002) was not detected in uninjured muscles, but strongly marked Myogenin-expressing differentiating satellite cells during muscle regeneration (Fig. S3 D). These data show that Wnt/β-catenin signaling is inactive during satellite cell quiescence, and becomes activated upon myogenic commitment. Thus, our results suggest that APC-depleted satellite cells present unscheduled aberrant activation of canonical Wnt signaling.

To test whether the phenotype of APC mutant cells was a direct consequence of canonical Wnt signaling overactivation, we simultaneously silenced APC and inhibited the Wnt/β-catenin pathway by combining APC and β-catenin siRNAs in vitro (Fig. 4 A). Using this strategy, we were able to completely ab-

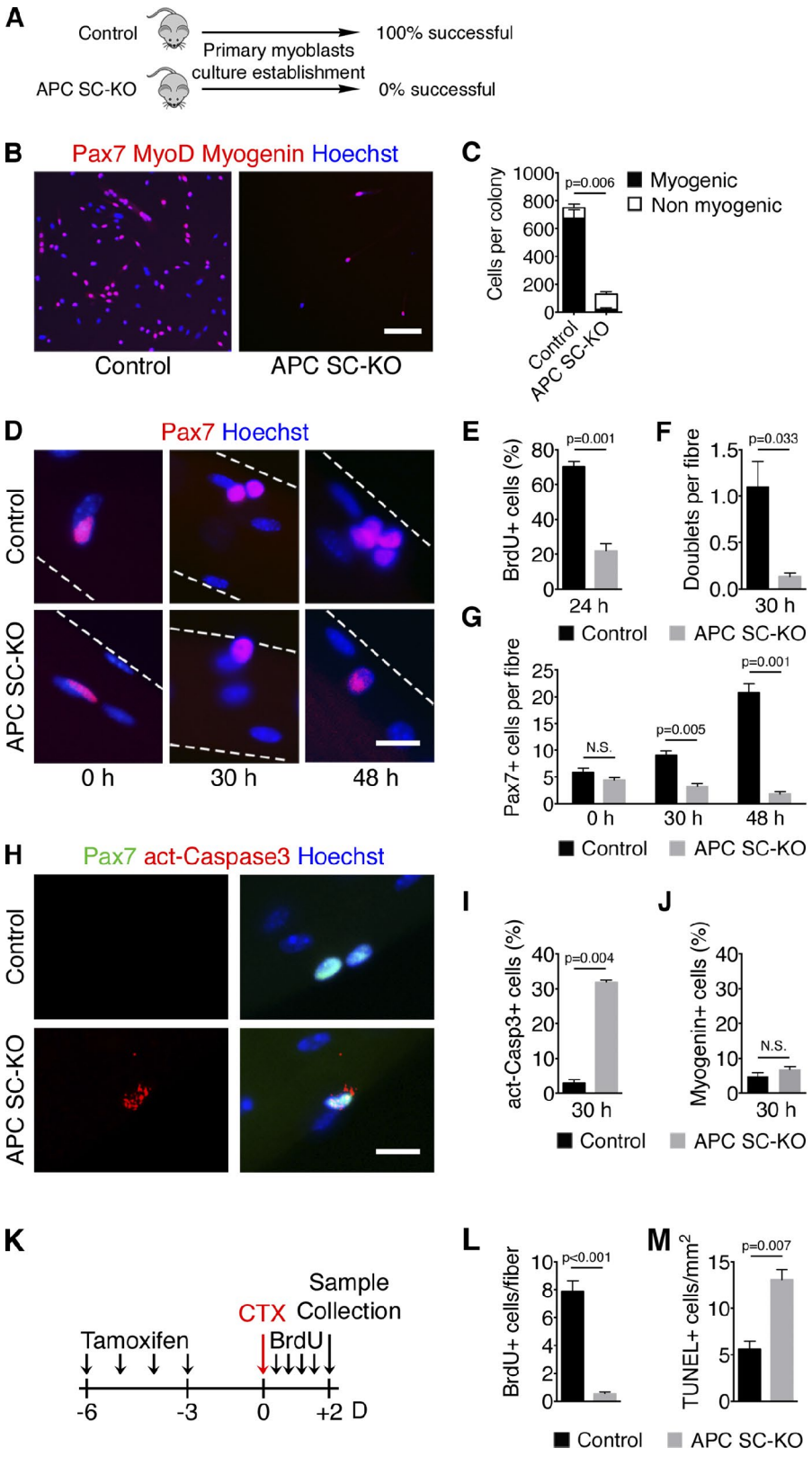

Figure 3. **APC-null satellite cells lose their myogenic potential and undergo apoptosis upon activation.** (A) Scheme of success ratio in generation of primary myoblasts culture from TM-treated control and APC SC-KO mice. (B) Pax7, MyoD, and Myogenin immunostaining on myogenic colonies obtained from single EDL fibers cultured on Matrigel for 7 d. (C) Quantification of the number of myogenic and nonmyogenic cells per colony obtained in B. P-value refers to the myogenic proportion. (D) Pax7 immunostaining on single EDL fibers isolated and fixed (0 h) or cultured in floating conditions for 30 or 48 h (broken lines indicate the underlying fiber). (E) Quantification of BrdU-incorporating satellite cells on EDL fibers after 24 h of culture. (F) Quantification of satellite cell doublets per fiber after 30 h of culture. (G) Quantification of total number of satellite cells per fiber after 0, 30, and 48 h of culture. (H) Pax7 and activated Caspase3 (act-Casp3) immunostaining on EDL single fibers after 30 h of culture. (I) Quantification of apoptotic satellite cells after 30 h of culture. (J) Quantification of the percentage of satellite cells on EDL fibers expressing Myogenin after 30 h of culture. (K) Schematic representation of the in vivo analysis of satellite cell proliferation and survival upon muscle injury. (L and M) Quantification of BrdU-incorporating satellite cells on regenerating EDL fibers (L) and of apoptotic cells by TUNEL staining on TA sections (M) 2 d after injury. Bars: (B) 100 µm; (D and H) 10 µm. Error bars indicate SEM. N.S., not significant ($P > 0.05$).

rogate transcriptional activation of the Wnt target gene Axin2 transcription by concomitant APC and β-catenin silencing (Fig. 4 B). We further observed the rescue of adequate G1-S checkpoint gene expression in APC;β-catenin double-silenced cells compared with cells only transfected with APC-targeting siRNA (Fig. 4 C). Strikingly, while simple APC silencing blocked BrdU incorporation and decreased the percentage of S-phase cells in proliferating primary myoblasts, silencing of both APC and β-catenin restored normal cell cycle progression (Fig. 4, D and E). In this experimental setup, we observed that the induction of programmed cell death in primary myoblasts after APC silencing requires β-catenin, as quantified by TUNEL

assay (Fig. 4 F). To determine whether β-catenin inactivation could compensate for APC loss in vivo, we conditionally deleted both genes in adult satellite cells. We used the $Pax7^{CreERT2}$ allele to recombine both APC floxed alleles along with one (SC APC-KO; βcat-HET) or two (SC APC-KO; βcat-KO) β-catenin floxed alleles (Brault et al., 2001) in adult mice. Strikingly, cardiotoxin-induced muscle regeneration was completely restored in TA muscles with APC;β-catenin double inactivated satellite cells (Fig. 4 G), as assessed by quantification of satellite cell numbers (Fig. 4 H) and regenerated fiber size (Fig. 4 I) 2 wk after injury. Importantly, recombination of only one β-catenin allele resulted in a partial rescue of APC genetic disruption. In this context, muscle regeneration occurred but satellite cells could not repopulate their niche, and the regenerated myofibers were smaller as compared with single or double inactivated TAs. These data demonstrate that cell cycle arrest and apoptosis after APC inactivation are triggered by β-catenin overactivation. Collectively, these experiments demonstrate that specific levels of canonical Wnt signaling are the major determinant of the observed phenotype in APC-SC-KO mice.

Conclusions

Here we report that APC is absolutely necessary for regenerative myogenesis. We show that APC inactivation in stem cells of a low-turnover tissue results in inhibition of proliferation and programmed cell death. This is in contrast with previous observations of several tissues with high turnover rate, in which APC acts as a tumor suppressor. Interestingly, these constantly renewing tissues have high tumor incidence, and it has been demonstrated, at least in some cases, that tumors derive from residing stem cells (Barker et al., 2009). In these cells, β-catenin hyperactivation after APC loss promotes unscheduled proliferation leading to neoplastic transformation (van de Wetering et al., 2002; Sansom et al., 2007). Importantly, this paradigm cannot be extended to skeletal muscle. Our data supports the evidence that tissue-specific stem cells have different susceptibility to cancer initiation, and suggest that these differences rely on tissue-specific functions of APC and the Wnt/β-catenin pathway.

Wnt/β-catenin signaling has previously been associated with skeletal muscle tissue repair. More specifically, regenerating muscle tissue expresses many Wnt ligands, and both the injection of recombinant Wnt3a protein (Brack et al., 2008) or the electroporation of a Wnt3a-expressing plasmid (Le Grand et al., 2009) perturbed the regeneration process by promoting myogenic lineage progression and differentiation. Further, expression of the constitutively active form of β-catenin, specifically in satellite cells, did not affect tissue regeneration, but rather prolonged the regenerative response (Murphy et al., 2014).

We observed that targeted APC gene disruption in satellite cells results in a massive up-regulation of canonical Wnt signaling that leads to complete failure of tissue regeneration. While unexpected, this phenotype is not contradictory with previous work since it is known that Wnt signaling influences self-renewing cells in a dosage-dependent fashion. Notably, Wnt signaling dosage modulates the capacity of embryonic stem cells to differentiate into the three main germ layers in vitro (Kielman et al., 2002) and regulates hematopoiesis in vivo (Luis et al., 2011). In animal models that develop cancer, different mutation types in different members of the Wnt pathway result in different signaling doses associated with specific tumors in susceptible tissues (Fodde and Smits, 2001). APC gene disruption represents the strongest possible activation of canonical Wnt signaling, as APC controls β-catenin protein stability in the cytoplasm, and also facilitates the repression of Wnt target genes at the chromatin level (Sierra et al., 2006).

Our results clearly indicate that different doses of β-catenin made available for Wnt signaling resulted in different cellular responses and, consequently, in different degrees of tissue regeneration. Full inactivation of canonical Wnt signaling by removal of β-catenin in APC-null satellite cells completely restored muscle tissue regeneration, whereas mild activation of the pathway after genetic disruption of only one allele of β-catenin in APC-null satellite cells resulted in an intermediate regeneration phenotype that can be compared with the minor regeneration defects observed after administration of exogenous Wnt proteins to the muscle tissue (Brack et al., 2008; Le Grand et al., 2009) and to the genetic activation of β-catenin in satellite cells (Murphy et al., 2014).

In this study we provide genetic evidence that, in the early phases of muscle tissue repair, canonical Wnt signaling is dampened by APC in satellite cells to allow their proper cell cycle entry and progression. Clinically, β-catenin or other canonical Wnt signaling regulators can be targeted (Liu et al., 2013) to drive the expansion of human satellite cells or induced pluripotent stem (iPS)-derived myogenic cells for skeletal muscle tissue repair with far-reaching medical impact.

Materials and methods

Mice

Experimental animal protocols were performed in accordance with the guidelines of the French Veterinary Department and approved by the University Paris-Descartes Ethical Committee for Animal Experimentation. All experiments were performed on age- and sex-matched mice, with an equal ratio of male to female mice. Generation and genotyping of the $Pax7^{CreERT2}$, $APC^{flox/flox}$, $\beta\text{-catenin}^{flox/flox}$, Z/EG, and $Axin2^{LacZ}$ lines have been described previously. The $Pax7^{CreERT2}$ allele is a null allele. The Cre-ERT2-IRES-DsRed cassette has been inserted in place of Pax7 exon 1 and 2. The APC^{flox} allele is a conditional null allele. The exon 14 of the APC gene was flanked with loxP sequences. The $\beta\text{-catenin}^{flox}$ allele is a conditional null allele. LoxP sequences were inserted in the β-catenin gene the before exon 2 and after exon 6. The Z/EG allele is a double reporter allele. The Z/EG transgene consists of the strong (pCAGGS) promoter directing expression of a loxP-flanked β-geo (lacZ/neomycin-resistance) fusion gene. Following is the coding sequence of the enhanced GFP. In this configuration, EGFP is expressed after Cre recombinase activity. The $Axin2^{LacZ}$ allele is a null allele. In-frame insertion of a nuclear-localized β-galactosidase (NLS-lacZ) gene into the endogenous Axin2 start codon resulted in deletion of the Axin2 exon 2. The $Axin2^{LacZ}$ mice were a gift from A.A. Chassot (Institut de Biologie Valrose, Nice, France).

Induction of Cre activity and cardiotoxin injury

I.p. injections of tamoxifen from MP Biomedicals at 5 µl per gram body weight of 20 mg/ml diluted in corn oil were administrated to 2-mo-old mice daily for 4 d before injury. For muscle injury experiments, mice were anaesthetized by i.p. injection of Ketamin-Xylazin (Centravet) at 10 µl per gram body weight of 80–10 mg/ml diluted in saline. Mouse legs were cleaned with alcohol and tibialis anterior muscles were injected with 35 µl of cardiotoxin solution (12 µM, diluted in saline; Latoxan) using an insulin needle (3/10 cc insulin syringe; BD). For in vivo proliferation assays, we used four i.p. injections of BrdU at 5 µl per gram of body weight of 10 mg/ml diluted in saline.

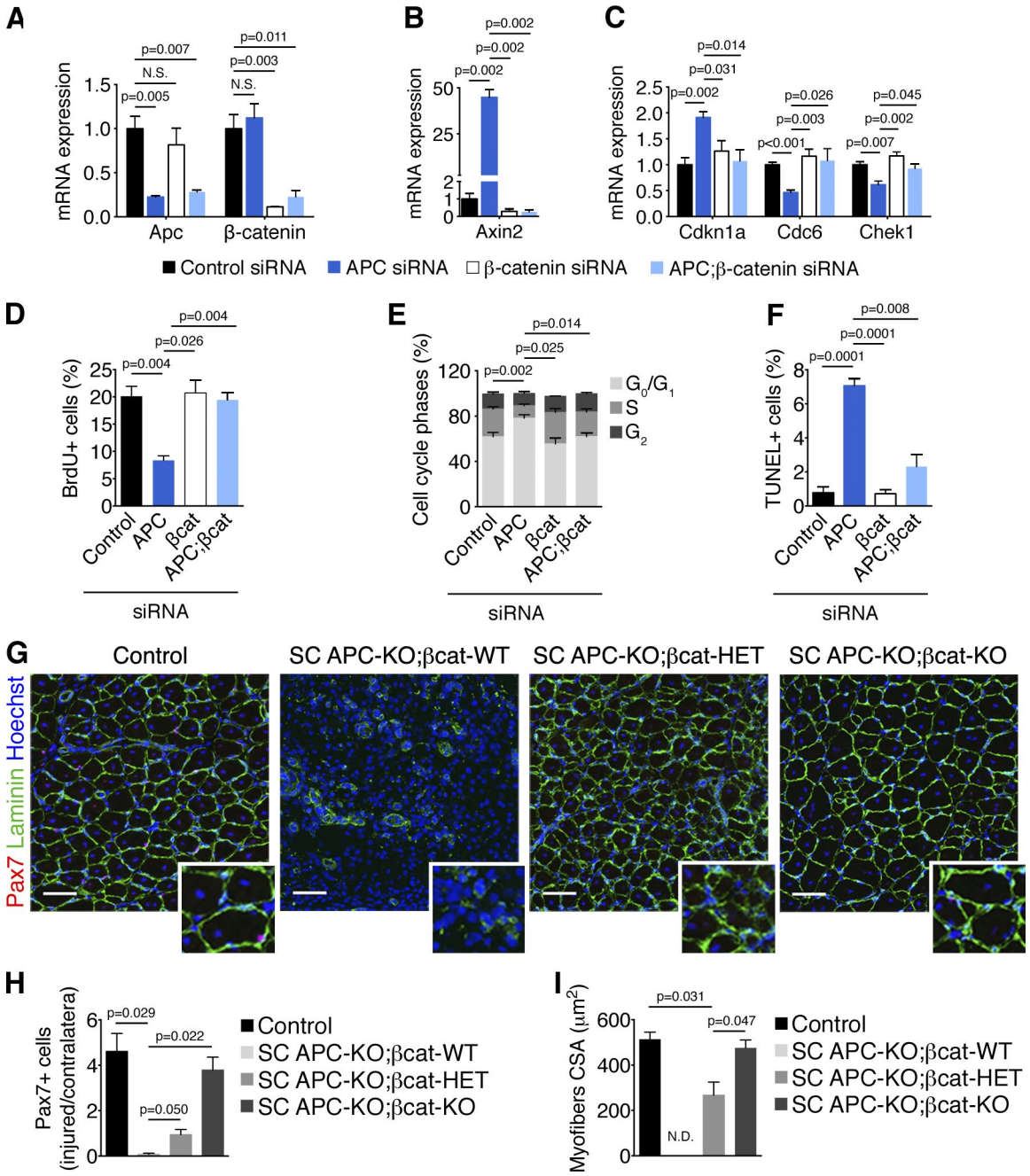

Figure 4. **APC controls satellite cell proliferation and survival by dampening Wnt/β-catenin signaling.** (A–C) RT-qPCR analysis of gene expression in proliferating primary myoblasts after siRNA treatment. Apc and β-catenin levels (A) show efficient reduction of the transcription of genes targeted by siRNA, whereas Axin2 levels (B) reveal that Wnt/β-catenin overactivation is blunted in APC;β-catenin double silenced cells. Cdkn1a induction and concomitant decrease of cdc6 and chek1 expression after APC knockdown reflect a G1/S arrest (C). (D) Quantification of BrdU+ primary myoblasts 48 h after siRNA transfection. (E) Distribution of primary myogenic cells in each cell cycle phase assessed by quantification of propidium iodide (PI) incorporation 48 h after siRNA transfection. P-value refers to S phase. (F) Quantification of apoptotic index by TUNEL staining on primary myoblasts 48 h after siRNA transfection. (G) TA cryosections 14 d after injury immunostained for Pax7 and Laminin. Nuclei were stained with Hoechst. Bars, 50 μm. Inset panels show 2× enlargements. (H) Quantification of sublaminar Pax7+ cells 14 d after injury (normalized by Pax7+ cells of noninjured TA). (I) Quantification of TA muscle fibers cross-sectional area (CSA) 14 d after injury. N.D., not determined. Error bars indicate SEM.

FACS-mediated cell isolation

Satellite cells were obtained from adult hindlimb muscles after enzymatic digestion followed by FACS purification. In brief, after dissection cells were digested for 1.5 h in digestion solution (2 mg/ml Collagenase A, 2.4 U/ml Dispase II, and 10 μg/ml DNase I, in HBSS; all from Roche). After digestion, cells were washed with wash buffer (0.2% BSA in HBSS; Gibco) and filtered twice; once with a 100-μm strainer and once with a 45-μm strainer (Corning). Cells were then stained with the following antibodies: rat CD31, rat CD45, rat TER119, rat Ly6A (SCA1), rat CD106 (eBioscience), and rat α7 integrin (R&D Systems) and sorted using a cell sorter (FACS Aria II; BD). Satellite cells were isolated as $CD31^{neg}$ $CD45^{neg}$ $Ter119^{neg}$ $Sca1^{neg}$ α7 $integrin^{pos}$. Fibroblasts were isolated as $CD31^{neg}$ $CD45^{neg}$ $Ter119^{neg}$ $Sca1^{pos}$ α7 $integrin^{neg}$. Genomic DNA from satellite cells and

fibroblasts was purified using QUICK-GDNA Microprep (Zymo Research). Sequences of the primers used for genotyping PCR were as follows: APC-Fwd, 5′-CTGTTCTGCAGTATGTTATCA-3′; APC-Rev-Lox, 5′-CTATGAGTCAACACAGGATTA-3′; APC-Rev-Del, 5′-TATAAGGGCTAACAGTCAATA-3′.

Histology and immunohistochemistry

For cryosections, skeletal muscles were embedded in Tissue-Tek O.C.T. Compound (Gentaur), frozen on 2-methylbutane–cooled liquid nitrogen, and processed for cryostat sectioning. 10-µm sections were collected from the midbelly of muscles. Immunohistochemistry was performed by fixation with 4% PFA/PBS, processing for antigen retrieval with the Antigen Unmasking Solution (Vector) at 95°C for 15 min in a thermostated microwave, permeabilization with 0.2% Triton X-100 in PBS, blocking with 5% heat-inactivated serum/0.2% Triton X-100/1% BSA/PBS, incubation with primary antibody overnight at 4°C, and then incubation with Alexa Fluor secondary antibodies for 1 h at room temperature. Nuclei were counterstained with Hoechst and slides were mounted in fluorescent mounting medium (Dako). Primary antibodies were as follows: mouse β-catenin (BD), goat Collagen Type I (SouthernBiotech), rabbit GFP (Life Technologies), rabbit Ki67 (Abcam), rabbit Laminin (Sigma-Aldrich), mouse MyoD (Dako), mouse embryonic-MyHC (Developmental Studies Hybridoma Bank), mouse Pax7 (DSHB), and rabbit Tcf4 (Cell Signaling Technology). The TUNEL reaction was performed by using the In situ cell death detection kit (Roche) according to the manufacturer's instructions for tissue cryosections.

Single myofibers isolation and primary myoblasts preparation

Single myofibers were isolated from the EDL muscle by Collagenase type I digestion and gentle triturating, as described previously (Le Grand et al., 2009). Isolated myofibers were cultured in suspension for up to 2 d in 6-well plates coated with horse serum to prevent fiber attachment. Alternatively, myofibers were left to adhere to Petri dishes coated with 20% Matrigel (BD) in DMEM (Life Technologies) and cultured for 7 d. Fibers were incubated in plating medium consisting of 15% FBS (Hyclone) and 1% chick embryo extract (Accurate Chemicals) in DMEM. For isolation of primary myoblasts, skeletal muscles of the hindlimbs of 6- to 8-wk-old mice were dissected, with care to take off as much fat and connective tissue as possible. Muscles were transferred to a sterile 6-cm Petri dish on ice, mulched into a smooth pulp, and incubated in CollagenaseB/DispaseII/$CaCl_2$ solution (respectively, 1.5 U/ml, 2.4 U/ml, and 2 M in DMEM; Roche). After a 15-min incubation at 37°C, the muscle pulp was triturated with heat-polished glass Pasteur pipettes, and this incubation/trituration step was repeated once. Tissue digestion was stopped with the addition of FBS, cells were filtered, washed twice with PBS, and resuspended in growth medium consisting of Ham's F10 (Life Technologies) supplemented with 20% FBS and 2.5 ng/µl of basic FGF (R&D systems). After 2 h of preplating in a noncoated 10-cm plate, the medium was transferred onto collagen-coated Petri dishes. Cultures were maintained in growth medium until cells reached 80% confluence. To enrich cell cultures in myoblasts and eliminate contaminating fibroblasts, cell dishes were tapped. Differential adhesion potential allows myoblasts to be detached and replated onto new plates.

RNA interference

Wild-type primary myoblasts were transfected with the following Silencer Select Pre-designed siRNA sequences (Life Technologies): APC, 5′-CAGCUGACCUAGCCCAUAAtt-3' β-catenin, 5′-CACUUGCAAUAAUUACAAAtt-3′. siRNA transfection was performed using Lipofectamine 2000 and OptiMEM (Life Technologies) according to the manufacturer's protocol.

Immunocytochemistry

Cells were fixed with 4% PFA/PBS, permeabilized with 0.2% Triton X-100/PBS, blocked with 5% heat-inactivated serum/PBS, incubated with primary antibody for at least 1 h, then incubated with Alexa Fluor secondary antibodies for 1 h. Nuclei were counterstained with Hoechst. Primary antibodies are as follows: rabbit APC (Abcam), mouse BrdU (Dako), rabbit activated-Caspase3 (Cell Signaling Technology), rabbit activated β-catenin (Cell Signaling Technology), mouse MyoD (Dako), rabbit Myogenin (Santa Cruz Biotechnology, Inc.), mouse Pax7 (Developmental Studies Hybridoma Bank), and rabbit PCNA (Bethyl Laboratories, Inc.). Secondary antibodies were conjugated with Alexa Fluor 488 or Alexa Fluor 550 fluorochromes. The TUNEL reaction was performed by using the In situ cell death detection kit (Roche) according to the manufacturer's instructions for adherent cell layers. For cell proliferation studies, cells were incubated for 40 min with culture medium containing 30 µM BrdU and processed for immunostaining with Pax7 and BrdU antibodies after fixation and treatment with 2N HCl for 20 min.

Image acquisition and quantitative analysis

Image acquisition and image analysis were performed at the Cochin Imaging Facility. Immunofluorescent stainings were analyzed with an Axiovert 200M microscope (Carl Zeiss) with 20× magnification equipped with a camera (CoolSNAP HQ) and with an AZ100 microscope (Nikon) with 5× magnification equipped with a high-resolution camera (Ds-Ri1; Nikon). Images were acquired at room temperature, the imaging medium used was Fluorescent Mounting Medium (Dako), and the fluorochromes used were Alexa Fluor 488 and Alexa Fluor 546 (Life Technologies). NIS-Element (Nikon), Metamorph (Molecular Devices), and Photoshop software (Adobe) were used for image acquisition and processing. All quantifications were done with ImageJ software.

Quantitative real-time PCR (qPCR)

Total RNA was extracted from either mouse tissue or cultured cells with TRIzol Reagent (Life Technologies) and treated with a DNA-free kit (Life Technologies) to remove any possible DNA contamination. cDNA was synthesized using the High-Capacity cDNA Reverse Transcription kit (Applied Biosystems) with 500 ng of RNA as input. Gene expression was assessed with a LightCycler 480 Real-Time PCR System (Roche) using LightCycler 480 SYBR green I Master (Roche) with specific primers. Transcript levels were determined by absolute quantification using a 4-point standard curve and relative gene expression was calculated by normalization against 18S and cyclophilin reference genes. Sequences of the primers used for real-time PCR were as follows: 18S-Fwd, 5′-GTAACCCGTTGACCCCATT-3′; 18S-Rev, 5′-CCATCCAATCGCTAGTAGCG-3′; APC-Fwd, 5′-GCAGCTACAGGGAAGTATTGAA-3′; APC-Rev, 5′-TCTCCTGAACGGCTGGATAC-3′; Axin2-Fwd, 5′-AAGAGAAGCGACCCAGTCAA-3′; Axin2-Rev, 5′-CTGCGATGCATCTCTCTCTG-3′; β-catenin-Fwd, 5′-ATGGAGCCGGACAGAAAAGC-3′; β-catenin-Rev, 5′-CTTGCCACTCAGGGAAGGA-3′; Cdc6-Fwd, 5′-CCCGGGATTGTGAAGTAAAA-3′; Cdc6-Rev, 5′-GGAGATAACCGGGGAGTGTT-3′; Cdkn1a-Fwd, 5′-TTGTCGCTGTCTTGCACTCT-3′; Cdkn1a-Rev, 5′-AATCTGTCAGGCTGGTCTGC-3′; Chek1-Fwd, 5′-TCGTGAACGCTTACTGAACAA-3′; Chek1-Rev, 5′-ACAGCTATCACTGGGCTGGT-3′; Cyclophilin-Fwd, 5′-AAGAAGATCACCATTTCCGACT-3′; Cyclophilin-Rev, 5′-TTACAGGACATTGCGAGC-3′; MyH3-Fwd, 5′-AGAGGAGAAGGCCAAAAGG-3′; MyH3-Rev, 5′-CCTTCCAGCTCAAACTCCAG-3′; Myogenin-Fwd, 5′-GAAAGTGAATGAGGCCTTCG-3′; Myogenin-Rev, 5′-ACGATGGACGTAAGGGAGTG-3′; Pax7-

Fwd, 5′-CTGGATGAGGGCTCAGATGT-3′; Pax7-Rev, 5′-GGTTAGCTCCTGCCTGCTTA-3′.

Microarray and bioinformatics

Total RNA was prepared from primary myoblasts using TRIzol Reagent (Life Technologies). After validation of the RNA quality with Bioanalyzer 2100 (using Agilent RNA6000 nano chip kit; Agilent Technologies), 50 ng of total RNA is reverse transcribed using the Ovation PicoSL WTA System (Nugen). In brief, the resulting double-strand cDNA is used for amplification based on single primer isothermal amplification (SPIA) technology. After purification according to the Nugen protocol, 5 µg of single-stranded DNA is used for generation of Sens Target DNA using Ovation Exon Module kit (Nugen). 2.5 µg of Sens Target DNA are fragmented and biotin labeled using an Encore Biotin Module kit (Nugen). After control of fragmentation using Bioanalyzer 2100, cDNA is then hybridized to GeneChip Mouse Gene 1.0 ST (Affymetrix) at 45°C for 17 h. After overnight hybridization, chips are washed on the fluidic station FS450 according to specific protocols (Affymetrix) and scanned using the GeneChip scanner 3000 7G (Affymetrix). The scanned images are then analyzed with Expression Console software (Affymetrix) to obtain raw data and metrics for Quality Controls. The observations of some of these metrics and the study of the distribution of raw data show no outlier experiments. Affymetrix probe-set data were normalized using the robust multi-array average (RMA) method (Irizarry et al., 2003) using R software (R Development Core Team, 2011). Gene expression levels were compared using one-way ANOVA. Lists of differentially expressed genes are presented in Table S2. Differentially expressed genes ($P < 0.01$, fold change > 1.5) were functionally annotated according to gene ontology terms, and enriched terms were calculated using DAVID (Huang et al., 2009; Table S1). Networks were generated with Ingenuity pathway analysis (Ingenuity Systems, http://www.ingenuity.com) using the Upstream Regulators and the Diseases&Functions tools that predict the activation status of signaling cascades and biological processes. The heat map with microarray data were created by using the matrix2png web interface (http://www.chibi.ubc.ca/matrix2png/bin/matrix2png.cgi).

Western blot analysis

Cells were lysed in RIPA buffer (Sigma-Aldrich) supplemented with Complete Protease Inhibitor Cocktail (Roche). Equal amounts of proteins were prepared with NuPAGE LDS Sample Buffer and Reducing Agent (Life Technologies), separated on NuPAGE Novex 3–8% Tris-Acetate Gels (Life Technologies), and transferred on nitrocellulose membranes (Bio-Rad Laboratories, Inc.). After blocking in 5% milk and 0.1% Tween-20/TBS, membranes were incubated with primary antibodies overnight and then with HRP-conjugated secondary antibodies for 1 h. Specific signals were detected with a chemiluminescence system (GE Healthcare). The following primary antibodies were used: rabbit APC (provided by K. Neufeld, University of Kansas, Lawrence, KS) and mouse HSC70 (Santa Cruz Biotechnology, Inc.).

Flow cytometric analysis for cell cycle

For cell cycle analysis, cells were trypsinized, collected in cold PBS, and fixed in 70% ethanol overnight at 4°C. After washing with PBS, cells were incubated with 50 µg/ml propidium iodide (Sigma-Aldrich), 50 µg/ml RNase A (Roche), and 0.1% Tween-20 in PBS for 15 min and then analyzed using an Accuri C6 flow cytometer (BD). Cell cycle phases were determined by using the cell cycle function of FlowJo software (Tristar).

Statistical analysis

Each histological analysis of adult skeletal muscle was performed on at least four samples per genotype. No randomization or blinding was used and no animals were excluded from analysis. For cell culture studies, at least three independent experiments were performed in duplicate and at least six random fields were imaged per sample. Data are presented as mean ± SEM. Differences between groups were tested for statistical significance using an unpaired two-tailed Student's *t* test. $P < 0.05$ was considered statistically significant. All statistical analyzes were performed using GraphPad Prism software.

Online supplemental material

Fig. S1 is a time-course histological analysis of muscle tissue regeneration in control and APC-SC-KO muscles. Fig. S2 illustrates the transcriptome results and the expression of PCNA by satellite cells. Fig. S3 show the up-regulation of canonical Wnt signaling in APC-deficient cells, and the activation of the pathway in satellite cells during muscle regeneration. Table S1 includes the Gene Ontology enrichment results. Table S2 is the list of genes that exhibit changes in expression after APC silencing. Online supplemental material is available at http://www.jcb.org/cgi/content/full/jcb.201501053/DC1.

Acknowledgments

We thank B. Chazaud, M. Buckingham, M. Rudnicki, P. Gilbert, and T. Cheung for critical reading of the manuscript. The authors greatly acknowledge B. Durel and P. Bourdoncle of the Cochin Imaging Facility. We thank members of the Cochin Institute genomic facility (S. Jacques and F. Dumont) for their technical and bioinformatics assistance. Microarray data have been deposited with the GEO Data Bank under the GSE57898 accession number.

This work was supported by funding from the Institut National de la Santé et de la Recherché Médicale, the Centre National de la Recherché Scientifique, the Agence National de Recherché (ANR Blanc, project RPV09108KKA; ANR Jeune Chercheur, project RPV13010KKA), and the Association Française contre les Myopathies. A. Parisi was supported by a fellowship from the Ministère de la Recherche et de l'Enseignement and a fellowship from the Fondation ARC pour la Recherche sur le Cancer.

The authors declare no competing financial interests.

Submitted: 14 January 2015
Accepted: 15 July 2015

References

Andreu, P., S. Colnot, C. Godard, S. Gad, P. Chafey, M. Niwa-Kawakita, P. Laurent-Puig, A. Kahn, S. Robine, C. Perret, and B. Romagnolo. 2005. Crypt-restricted proliferation and commitment to the Paneth cell lineage following Apc loss in the mouse intestine. *Development.* 132:1443–1451. http://dx.doi.org/10.1242/dev.01700

Barker, N., R.A. Ridgway, J.H. van Es, M. van de Wetering, H. Begthel, M. van den Born, E. Danenberg, A.R. Clarke, O.J. Sansom, and H. Clevers. 2009. Crypt stem cells as the cells-of-origin of intestinal cancer. *Nature.* 457:608–611. http://dx.doi.org/10.1038/nature07602

Brack, A.S., I.M. Conboy, M.J. Conboy, J. Shen, and T.A. Rando. 2008. A temporal switch from notch to Wnt signaling in muscle stem cells is necessary for normal adult myogenesis. *Cell Stem Cell.* 2:50–59. http://dx.doi.org/10.1016/j.stem.2007.10.006

Brault, V., R. Moore, S. Kutsch, M. Ishibashi, D.H. Rowitch, A.P. McMahon, L. Sommer, O. Boussadia, and R. Kemler. 2001. Inactivation of the β-catenin gene by *Wnt1-Cre*-mediated deletion results in dramatic brain malformation and failure of craniofacial development. *Development.* 128:1253–1264.

Chang, C.C., S.T. Chuang, C.Y. Lee, and J.W. Wei. 1972. Role of cardiotoxin and phospholipase A in the blockade of nerve conduction and depolarization of skeletal muscle induced by cobra venom. *Br. J. Pharmacol.* 44:752–764. http://dx.doi.org/10.1111/j.1476-5381.1972.tb07313.x

Clevers, H., and R. Nusse. 2012. Wnt/β-catenin signaling and disease. *Cell.* 149:1192–1205. http://dx.doi.org/10.1016/j.cell.2012.05.012

Colnot, S., T. Decaens, M. Niwa-Kawakita, C. Godard, G. Hamard, A. Kahn, M. Giovannini, and C. Perret. 2004. Liver-targeted disruption of *Apc* in mice activates β-catenin signaling and leads to hepatocellular carcinomas. *Proc. Natl. Acad. Sci. USA.* 101:17216–17221. http://dx.doi.org/10.1073/pnas.0404761101

Fodde, R., and R. Smits. 2001. Disease model: familial adenomatous polyposis. *Trends Mol. Med.* 7:369–373. http://dx.doi.org/10.1016/S1471-4914(01)02050-0

Fodde, R., R. Smits, and H. Clevers. 2001a. APC, signal transduction and genetic instability in colorectal cancer. *Nat. Rev. Cancer.* 1:55–67. http://dx.doi.org/10.1038/35094067

Fodde, R., J. Kuipers, C. Rosenberg, R. Smits, M. Kielman, C. Gaspar, J.H. van Es, C. Breukel, J. Wiegant, R.H. Giles, and H. Clevers. 2001b. Mutations in the APC tumour suppressor gene cause chromosomal instability. *Nat. Cell Biol.* 3:433–438. http://dx.doi.org/10.1038/35070129

Günther, S., J. Kim, S. Kostin, C. Lepper, C.-M. Fan, and T. Braun. 2013. Myf5-positive satellite cells contribute to Pax7-dependent long-term maintenance of adult muscle stem cells. *Cell Stem Cell.* 13:590–601. http://dx.doi.org/10.1016/j.stem.2013.07.016

Huang, W., B.T. Sherman, and R.A. Lempicki. 2009. Systematic and integrative analysis of large gene lists using DAVID bioinformatics resources. *Nat. Protoc.* 4:44–57. http://dx.doi.org/10.1038/nprot.2008.211

Irizarry, R.A., B.M. Bolstad, F. Collin, L.M. Cope, B. Hobbs, and T.P. Speed. 2003. Summaries of Affymetrix GeneChip probe level data. *Nucleic Acids Res.* 31:e15. http://dx.doi.org/10.1093/nar/gng015

Kielman, M.F., M. Rindapää, C. Gaspar, N. van Poppel, C. Breukel, S. van Leeuwen, M.M. Taketo, S. Roberts, R. Smits, and R. Fodde. 2002. Apc modulates embryonic stem-cell differentiation by controlling the dosage of β-catenin signaling. *Nat. Genet.* 32:594–605. http://dx.doi.org/10.1038/ng1045

Le Grand, F., A.E. Jones, V. Seale, A. Scimè, and M.A. Rudnicki. 2009. Wnt7a activates the planar cell polarity pathway to drive the symmetric expansion of satellite stem cells. *Cell Stem Cell.* 4:535–547. http://dx.doi.org/10.1016/j.stem.2009.03.013

Lepper, C., S.J. Conway, and C.-M. Fan. 2009. Adult satellite cells and embryonic muscle progenitors have distinct genetic requirements. *Nature.* 460:627–631. http://dx.doi.org/10.1038/nature08209

Lepper, C., T.A. Partridge, and C.-M. Fan. 2011. An absolute requirement for Pax7-positive satellite cells in acute injury-induced skeletal muscle regeneration. *Development.* 138:3639–3646. http://dx.doi.org/10.1242/dev.067595

Liu, J., S. Pan, M.H. Hsieh, N. Ng, F. Sun, T. Wang, S. Kasibhatla, A.G. Schuller, A.G. Li, D. Cheng, et al. 2013. Targeting Wnt-driven cancer through the inhibition of Porcupine by LGK974. *Proc. Natl. Acad. Sci. USA.* 110:20224–20229. http://dx.doi.org/10.1073/pnas.1314239110

Luis, T.C., B.A.E. Naber, P.P.C. Roozen, M.H. Brugman, E.F.E. de Haas, M. Ghazvini, W.E. Fibbe, J.J.M. van Dongen, R. Fodde, and F.J.T. Staal. 2011. Canonical wnt signaling regulates hematopoiesis in a dosage-dependent fashion. *Cell Stem Cell.* 9:345–356. http://dx.doi.org/10.1016/j.stem.2011.07.017

Lustig, B., B. Jerchow, M. Sachs, S. Weiler, T. Pietsch, U. Karsten, M. van de Wetering, H. Clevers, P.M. Schlag, W. Birchmeier, and J. Behrens. 2002. Negative feedback loop of Wnt signaling through upregulation of conductin/axin2 in colorectal and liver tumors. *Mol. Cell. Biol.* 22:1184–1193. http://dx.doi.org/10.1128/MCB.22.4.1184-1193.2002

McCartney, B.M., and I.S. Näthke. 2008. Cell regulation by the Apc protein: Apc as master regulator of epithelia. *Curr. Opin. Cell Biol.* 20:186–193. http://dx.doi.org/10.1016/j.ceb.2008.02.001

Morin, P.J., A.B. Sparks, V. Korinek, N. Barker, H. Clevers, B. Vogelstein, and K.W. Kinzler. 1997. Activation of β-catenin-Tcf signaling in colon cancer by mutations in β-catenin or APC. *Science.* 275:1787–1790. http://dx.doi.org/10.1126/science.275.5307.1787

Moseley, J.B., F. Bartolini, K. Okada, Y. Wen, G.G. Gundersen, and B.L. Goode. 2007. Regulated binding of adenomatous polyposis coli protein to actin. *J. Biol. Chem.* 282:12661–12668. http://dx.doi.org/10.1074/jbc.M610615200

Murphy, M.M., A.C. Keefe, J.A. Lawson, S.D. Flygare, M. Yandell, and G. Kardon. 2014. Transiently active Wnt/β-catenin signaling is not required but must be silenced for stem cell function during muscle regeneration. *Stem Cell Rev.* 3:475–488. http://dx.doi.org/10.1016/j.stemcr.2014.06.019

Nelson, S., and I.S. Näthke. 2013. Interactions and functions of the adenomatous polyposis coli (APC) protein at a glance. *J. Cell Sci.* 126:873–877. http://dx.doi.org/10.1242/jcs.100479

Novak, A., C. Guo, W. Yang, A. Nagy, and C.G. Lobe. 2000. Z/EG, a double reporter mouse line that expresses enhanced green fluorescent protein upon Cre-mediated excision. *Genesis.* 28:147–155. http://dx.doi.org/10.1002/1526-968X(200011/12)28:3/4<147::AID-GENE90>3.0.CO;2-G

R Development Core Team. 2011. R: A Language and Environment for Statistical Computing. Vienna, Austria: the R Foundation for Statistical Computing. Available at http://www.R-project.org/ (accessed July 11, 2005).

Sansom, O.J., K.R. Reed, A.J. Hayes, H. Ireland, H. Brinkmann, I.P. Newton, E. Batlle, P. Simon-Assmann, H. Clevers, I.S. Nathke, et al. 2004. Loss of Apc in vivo immediately perturbs Wnt signaling, differentiation, and migration. *Genes Dev.* 18:1385–1390. http://dx.doi.org/10.1101/gad.287404

Sansom, O.J., V.S. Meniel, V. Muncan, T.J. Phesse, J.A. Wilkins, K.R. Reed, J.K. Vass, D. Athineos, H. Clevers, and A.R. Clarke. 2007. Myc deletion rescues Apc deficiency in the small intestine. *Nature.* 446:676–679. http://dx.doi.org/10.1038/nature05674

Seale, P., L.A. Sabourin, A. Girgis-Gabardo, A. Mansouri, P. Gruss, and M.A. Rudnicki. 2000. Pax7 is required for the specification of myogenic satellite cells. *Cell.* 102:777–786. http://dx.doi.org/10.1016/S0092-8674(00)00066-0

Sierra, J., T. Yoshida, C.A. Joazeiro, and K.A. Jones. 2006. The APC tumor suppressor counteracts β-catenin activation and H3K4 methylation at Wnt target genes. *Genes Dev.* 20:586–600. http://dx.doi.org/10.1101/gad.1385806

van de Wetering, M., E. Sancho, C. Verweij, W. de Lau, I. Oving, A. Hurlstone, K. van der Horn, E. Batlle, D. Coudreuse, A.P. Haramis, et al. 2002. The β-catenin/TCF-4 complex imposes a crypt progenitor phenotype on colorectal cancer cells. *Cell.* 111:241–250. http://dx.doi.org/10.1016/S0092-8674(02)01014-0

Watanabe, T., S. Wang, J. Noritake, K. Sato, M. Fukata, M. Takefuji, M. Nakagawa, N. Izumi, T. Akiyama, and K. Kaibuchi. 2004. Interaction with IQGAP1 links APC to Rac1, Cdc42, and actin filaments during cell polarization and migration. *Dev. Cell.* 7:871–883. http://dx.doi.org/10.1016/j.devcel.2004.10.017

Yin, H., F. Price, and M.A. Rudnicki. 2013. Satellite cells and the muscle stem cell niche. *Physiol. Rev.* 93:23–67. http://dx.doi.org/10.1152/physrev.00043.2011